INDIAN JOURNAL OF SCIENCE AND TECHNOLOGY

ORIGINAL ARTICLE

Check for updates

OPEN ACCESS

Received: 01/05/2026

Accepted: 27/07/2026

Published: 17/08/2026

Citation: Roopa KV, Subramanya K (2026) Enhancement of Optical, Dielectric and Electrical Transport Properties in $CoCl_2$-Doped PEO Polymer Electrolyte Films by Gamma Irradiation for Optoelectronic Applications. Indian Journal of Science and Technology 19(29): 2109-2118. https://doi.org/10.17485/IJST/v19i29.713

* **Corresponding author**.

subbuk17@gmail.com

Funding: None

Competing Interests: None

Copyright: © 2026 Roopa & Subramanya. This is an open access article distributed under the terms of the Creative Commons Attribution License, which permits unrestricted use, distribution, and reproduction in any medium, provided the original author and source are credited.

Published By Indian Society for Education and Environment (iSee)

ISSN
Print: 0974-6846
Electronic: 0974-5645

Enhancement of Optical, Dielectric and Electrical Transport Properties in $CoCl_2$-Doped PEO Polymer Electrolyte Films by Gamma Irradiation for Optoelectronic Applications

K V Roopa[1], K Subramanya[1]*

1 Department of PG Studies and Research in Physics, Kuvempu University, Shankaraghatta, Shivamogga, 577451, Karnataka, India

Abstract

Objectives: This study investigates physical properties such as structural, optical, dielectric, and electrical properties of cobaltous chloride ($CoCl_2$)-doped polyethylene oxide (PEO) Polymer Electrolyte Films for optoelectronic applications upon γ-irradiation. **Method:** PEO–$CoCl_2$ films with varying dopant concentrations were prepared using the solution casting technique. Among these selected samples were exposed to different doses of γ-irradiation to induce controlled modifications. Structural properties modifications were analyzed using X-ray diffraction (XRD) and Fourier transform infrared (FTIR) spectroscopy. Optical properties were evaluated using UV–Visible spectroscopy, while dielectric and electrical properties were studied through dielectric and AC conductivity measurements. **Findings:** Structural properties modifications were analyzed using X-ray diffraction (XRD) and Fourier transform infrared (FTIR) spectroscopy data with slight shift in 2θ along with slightly decreased in peak width from 0.307 to 0.049 and reduced crystallinity confirming a transition toward an amorphous phase along with chain scission and cross-linking irradiation as a result of γ-irradiation. The incorporation of $CoCl_2$ transformed semicrystalline, PEO into a more amorphous phase due to coordination between Co^{2+} ions and polymer chains, which was further enhanced by γ-irradiation through chain scission and cross-linking. Optical analysis revealed a significant reduction in the direct band gap reaching 1.30 eV for irradiated films, indicating improved optical conductivity along with shift in the peak to red region. Dielectric studies showed increased polarization and reduced relaxation time, while AC conductivity results confirmed enhanced charge carrier mobility. These improvements are attributed to the dissociation of $CoCl_2$ into mobile ions, facilitating hopping conduction within the polymer matrix. **Novelty:** This work provides quantitative evidences, the combined effect of $CoCl_2$ doping and γ-irradiation significantly enhances ion transport and electrical performance of PEO-based composites. The developed films demonstrate shows strong potential for use in flexible electrodes and low-energy optoelectronic devices.

Keywords: Polymer electrolyte films; Gamma-irradiation; AC conductivity; optical band gap; dielectric properties

1 Introduction

Conventional metallic thin films have been widely used as conductive layers due to their high charge transport efficiency because of their high sensitivity in conductive application [1], [2]. However, their inherent rigidity, density and poor mechanical applicability restricts their usage in flexible and solid-state electrochemical devices. Conversely, polymer electrolytes have emerged as viable substitute owing to their flexibility, lightweight nature, durability, mechanical stability, easy synthesis and tunable ionic conductivity [3], [4]. Among various fabrication techniques, solution casting remains particularly attractive due to its simplicity, low cost, multiple devices at a short time, and ability to produce uniform thin films with controlled thickness.

Polyethylene oxide (PEO) is one of the most extensively studied organic host polymers for solid polymer electrolytes due to its semicrystalline nature, good film forming ability, simple structure, long chain polymer and ability to solvate ionic species with ether oxygen coordination [5]. Nevertheless, its ionic conductivity is often limited by the presence of species of charge carrier domains, which hinder by segmental energy produced by charge species and ion mobility. To conquer this limitation, incorporation of transition metal salts such as cobaltous chloride ($CoCl_2$) has been widely explored, as it enhances ionic transport by increasing the number of charge carriers and support ion–polymer interactions. In supplementary, γ-irradiation has emerged as an effective non-chemical approach for tailoring in altering polymer structure through chain scission and cross-linking processes, resulting in increased amorphization, defect formation, and free volume, all of which are favorable for ion transport [6]. Despite these advances, a systematic understanding of the combined influence of metal salt doping and γ-irradiation on the structural evolution and ion transport mechanisms in PEO-based systems remains limited.

In this work, $CoCl_2$-doped PEO films are prepared via solution casting and systematically investigated under different γ-irradiation doses. Structural characterization using X-ray diffraction (XRD) and Fourier transform infrared spectroscopy (FTIR) examined shows reduction in crystallinity and significant modification of polymer–ion coordination. Optical properties, band gap variations were analyzed using Tauc's method, while electrical behavior is examined through AC conductivity and dielectric measurements over a range of frequencies. The results reveal that γ-irradiation induces localized defect states and structural disorder, which act as hopping sites for charge carriers, thereby facilitating ion migration within the polymer matrix. Furthermore, the dissociation of $CoCl_2$ into Co^{2+} and Cl^- ions contribute to increased charge carrier density, enhancing the overall conductivity [7], [8].

Recent studies have road mapped improved physical properties of polymer electrolyte through either metal salt doping or irradiation technique implied individually. However, the systematic investigation addressing the combined effect of dopant-induced charge carriers and irradiation-induced amorphization, structural modifications result in a significant improvement in ionic conductivity, dielectric response, and charge transport dynamics. These findings highlight the essential component induced defect-engineered, amorphization in optimizing polymer electrolyte performance. In particular the correlation between irradiation-induced amorphization, localized defect states, enhanced ion hopping conduction has fully established [9].

Overall, this study demonstrates that controlled γ-irradiation is an effective strategy for tuning the structural and electrical properties of polymer electrolytes. The developed γ-irradiation $CoCl_2$-doped PEO films exhibit strong potential for applications in solid-state electrochemical systems, flexible energy storage systems, and modernized ion-conducting materials.

2 Methodology

2.1 Materials

Polyethylene oxide (PEO(C2H4O)n, average molecular weight 5.6×10^6 g/mol, Merck) was used as the host polymer. Cobaltous chloride ($CoCl_2$, Mw = 237.93 g/mol, SD Fine Ltd.) served as the dopant to introduce mobile ionic species into the polymer matrix. Methanol (Mw = 32.04 g/mol, SD Fine Ltd.) was used as the solvent. All chemicals were used as received without further purification.

2.2 Preparation of PEO–$CoCl_2$ Composite Films

PEO–$CoCl_2$ composite films were achieved via the solution casting technique. A calculated amount of PEO 4g was dissolved in methanol 25ml under continuous magnetic stirring at room temperature 40C until a clear and homogeneous viscous solution was obtained. Subsequently, $CoCl_2$ was added in predetermined weight percentages (e.g., 10 wt%, i.e, 0.4gm) and stirred for 20 hours, ensuring complete disintegration and uniform dispersion.

The resulting solution was cast onto clean, leveled glass Petri dishes and allowed to evaporate slowly under ambient conditions. The dried films were further kept under vacuum/desiccation to remove residual solvent. The obtained free-standing films were carefully peeled off and stored in airtight conditions for further characterization.

2.3 Gamma-Irradiation

The prepared PEO–$CoCl_2$ films were subjected to γ-irradiation at different doses (e.g., 25 and 50 kGy) using a standard gamma radiation source. Irradiation was carried out under controlled conditions at room temperature. Both irradiated and pristine samples were preserved for comparative analysis to evaluate irradiation-induced modifications.

2.4 Characterization Techniques

The structural properties of the films were examined using X-ray diffraction (XRD) to assess crystallinity, phase transitions, and crystallite size. Fourier transform infrared (FTIR) spectroscopy was employed to identify functional groups and investigate polymer–ion interactions.

Optical properties were analyzed using UV–Visible spectroscopy in the wavelength range of 200–800 nm. The absorption coefficient was calculated, and the optical band gap was determined using Tauc's relation. Activation energy was evaluated using Arrhenius analysis.

Electrical and dielectric properties were studied using impedance spectroscopy over a wide frequency range. AC conductivity, dielectric constant (ε'), and dielectric loss (ε'') were calculated. Nyquist plots were used to determine bulk resistance and to elucidate charge transport mechanisms within the polymer electrolyte films.

3 Results and Discussion

3.1 X-ray Diffraction (XRD) Analysis

The structural evolution of pure PEO and $CoCl_2$-doped PEO films, before and after γ-irradiation, was analyzed using XRD (Figure 1). Pristine PEO exhibits sharp diffraction peaks, confirming its semicrystalline nature[10]. Upon $CoCl_2$ doping, a reduction in peak intensity is observed, indicating disruption of crystalline regions due to polymer–salt interactions and coordination between Co^{2+} ions and ether oxygen groups[11].

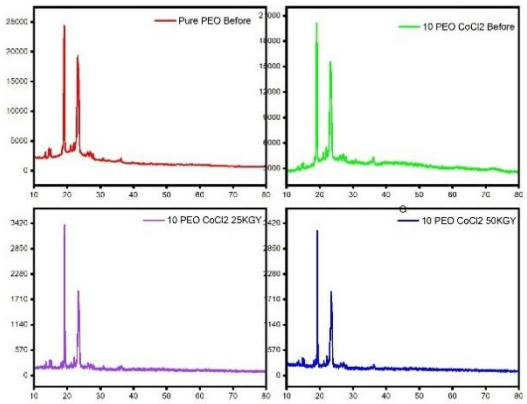


Fig 1. X-ray diffraction (XRD) patterns of pure PEO and $CoCl_2$-doped PEO films before and after γ-irradiation.

Gamma-irradiation leads to a further decrease in peak intensity and noticeable peak broadening, indicating enhanced amorphization. This is attributed to chain scission and cross-linking processes that increase structural disorder and reduce long-range order[12]. The resulting increase in amorphous content promotes segmental chain mobility, facilitating ion transport.

The broadened peaks in irradiated films suggest reduced crystallite size and increased microstrain, consistent with Scherrer analysis. Increased full width at half maximum (FWHM) values further support the formation of smaller crystallites and structural defects. Additionally, the structural transition from the monoclinic phase of pure PEO to a more disordered phase confirms the formation of polymer–salt complexes[13].

$$d = \frac{\lambda}{2sin\theta} \tag{1}$$

Using Scherer formula equation 2, average crystallite size is calculated,

$$L = \frac{k\lambda}{\beta cos\theta} \tag{2}$$

Structural parameters inter-crystallite separation (R) is calculated using equation 3,

$$R = \frac{5\lambda}{8sin\theta} \tag{3}$$

Average lattice parameter is calculated using equation 4,

$$P = \frac{\lambda}{2\sqrt{k}} \tag{4}$$

where $\lambda = 1.5 \times 10^{-10}$ m, k=0.9 and β is the full width at half maximum (FWHM). The XRD parameters for samples with varying weight percentages of $CoCl_2$ dopant are shown in Table 1.

Table 1. Structural parameters obtained from XRD analysis, including 2θ, d-spacing, crystallite size (L), inter-crystallite separation (R), lattice parameter (P), and FWHM for pure and $CoCl_2$-doped PEO films under different γ-irradiation doses.

Sample	2θ degree	d- $= \frac{\lambda}{2sin\theta}$ **A⁰m**	FWHM	$L = \frac{k\lambda}{\beta cos\theta}$ **nm**	$R = \frac{5\lambda}{8sin\theta}$ **A⁰m**	$P = \frac{\lambda}{2\sqrt{k}}$ **A⁰m**
Pure PEO	13.46	6.57	0.127	1.07-1.10	7.99	7.0-9.33
	19.10 23.19	4.64	0.204		5.65	
	36.21	3.83	0.127		4.66	
		2.48	0.307		3.01	
10%	13.44	6.58	0.09	1.07-1.12	8.01	6.75-9.33
Before	19.09	4.64	0.204		5.65	
	23.18	3.83	0.127		4.66	
	36.16	2.48	0.307		3.02	
10%	13.50	6.55	0.001	1.07-1.09	7.97	9.2-11.35
25KGy	19.23	4.61	0.123		5.61	
	23.34	3.81	0.103		4.63	
	36.31	2.47	0.158		3.00	
10%	13.65	6.48	0.208	1.07-1.09	7.88	7.02
50KGy	19.24	4.61	0.144		5.60	
	23.34	3.81	0.103		4.63	
	36.34	2.47	0.049		3.00	

3.2 Fourier Transform Infrared (FTIR) Spectroscopy

The structural modifications in pure PEO and $CoCl_2$-doped PEO films before and after γ-irradiation were analyzed using FTIR spectroscopy (Figure 2). The spectrum of pristine PEO shows characteristic bands corresponding to C–H wagging, CH_2 symmetric and asymmetric stretching, and C–C stretching, confirming its semicrystalline structure[14].

Upon $CoCl_2$ doping and γ-irradiation, noticeable shifts, intensity changes, and peak broadening are observed, indicating significant alterations in the polymer matrix. The O–H stretching band becomes broader and less intense after irradiation, suggesting disruption of hydrogen bonding and modification of the local chemical environment[3]. A broad absorption band in the 3300–2300 cm^{-1} region is attributed to overlapping O–H and C–H vibrations, while features around 2700–2800 cm^{-1}.

Additionally, changes in the fingerprint region confirm the formation of Co–O and Co–Cl bonds, evidencing coordination between Co^{2+} ions and the polymer backbone[15]. Increasing γ-irradiation dose further enhances peak broadening and reduces intensity, indicating increased amorphization and bond reorganization. These spectral changes support the formation of polymer–salt complexes and increased structural disorder, which facilitate ionic transport.

3.3 UV–Visible Spectroscopy

The UV–Visible absorption spectra of pure and $CoCl_2$-doped PEO films before and after γ-irradiation are shown in Figure 3. The doped films exhibit a broad absorption band in the 600–700 nm region, attributed to d–d transitions of Co^{2+} ions, confirming Co–O coordination within the polymer matrix[16].

Following γ-irradiation, additional absorption features appear around 437 nm, corresponding to n$\rightarrow\sigma^{\star}$ and $\sigma\rightarrow\sigma^{\star}$ transitions, indicating irradiation-induced chain scission and formation of localized states[17]. The presence of unsaturated

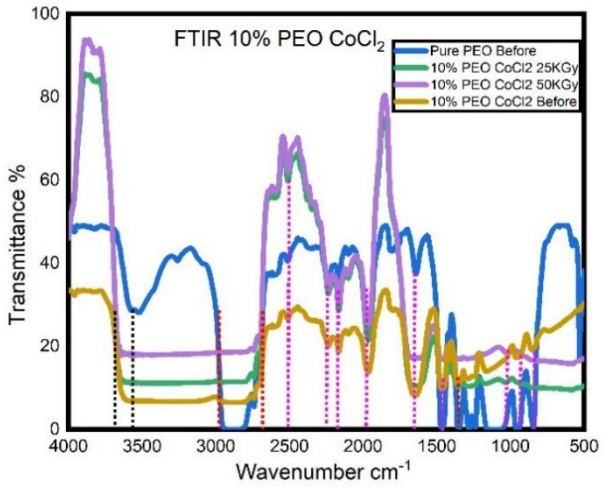


Fig 2. FTIR spectra of pure and $CoCl_2$-doped PEO films before and after γ-irradiation.

bonds (C=C and C≡C) further contributes to n→σ^* and $\pi \rightarrow \pi^*$ transitions. These spectral changes reflect increased structural disorder and defect formation. Overall, γ-irradiation enhances optical absorption and reduces transmittance, suggesting improved optical conductivity and stronger light–matter interaction in the doped films.

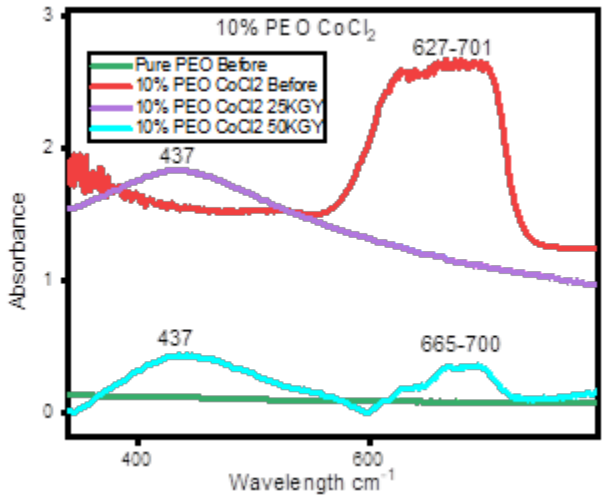


Fig 3. UV–Visible absorption spectra of pure and $CoCl_2$-doped PEO films before and after γ-irradiation.

The absorption coefficient (α) was calculated using Eq. (5),

$$\alpha = \frac{2.303 * A}{t} \tag{5}$$

and the optical band gap was determined using Tauc's relation (Eq. 6)

$$\alpha h\nu = A(h\nu - E_g)^n \tag{6}$$

The direct band gap (n = 2) and indirect band gap values are illustrated in Figs. 4, respectively.

For pure PEO, the direct band gap decreases from 4.05eV to 2.0eV after γ-irradiation, indicating increased structural disorder. In $CoCl_2$-doped films, the band gap further reduces to 1.68eV and reaches a minimum of 1.30eV at 25kGy, reflecting

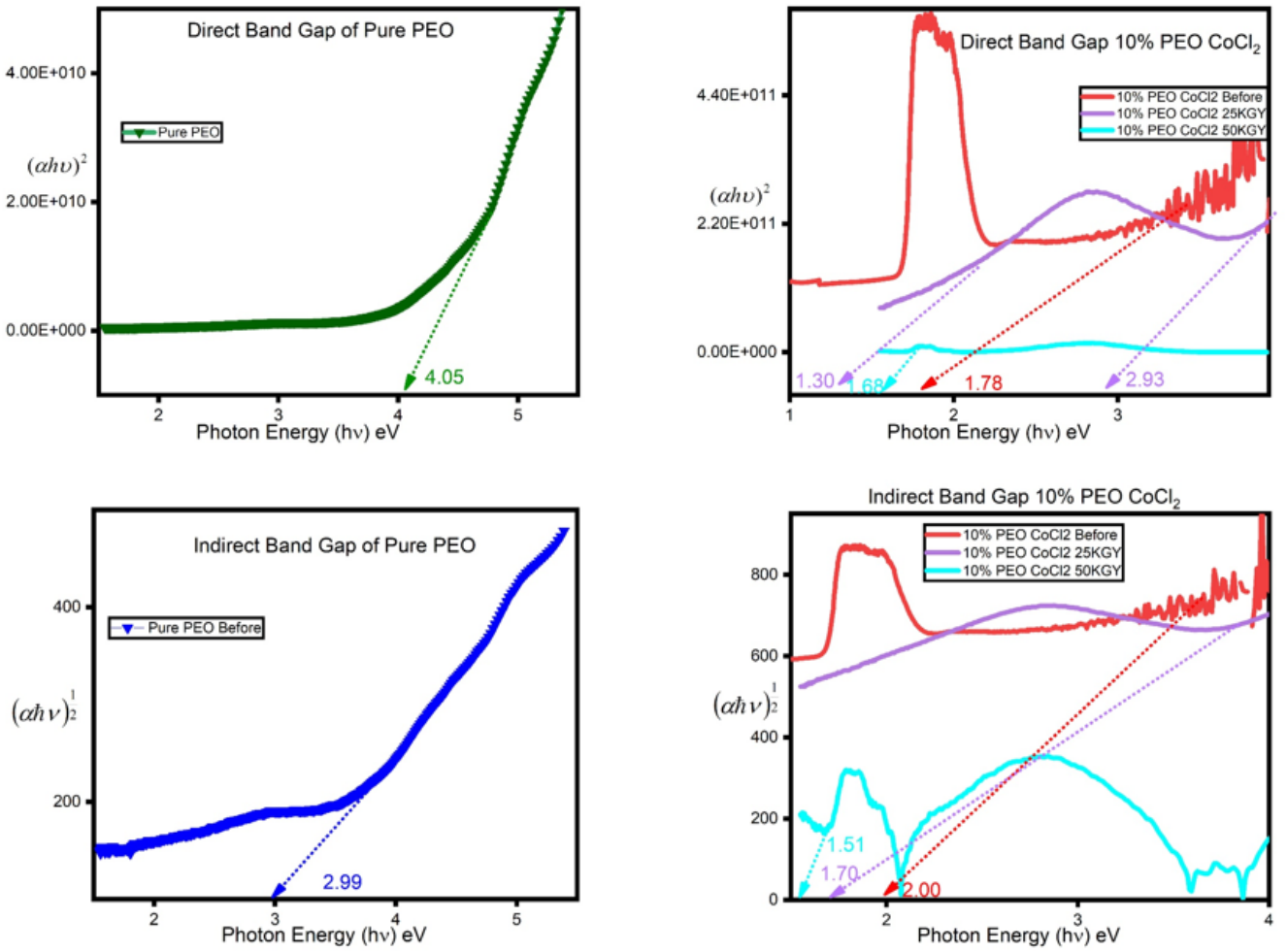


Fig 4. Variation of direct and indirect band gap energy for pure and $CoCl_2$-doped PEO films under different γ-irradiation doses.

enhanced defect formation and reduced energy required for electronic transitions. A similar decreasing trend is observed for the indirect band gap, confirming the formation of localized states within the band structure[18].

The extinction coefficient and refractive index were calculated using Eqs. (7) and (8),

$$\text{Extinction Coefficient, } k = \frac{\alpha\lambda}{4\pi} \tag{7}$$

$$\text{Refractive index, } n = \sqrt{\frac{(1+R)^2 - k^2}{(1-R)^2 + k^2}} \tag{8}$$

respectively, and the variation in refractive index with irradiation dose is shown in Figure 5. An increase in refractive index indicates enhanced optical density and stronger photon–material interaction, which is beneficial for optoelectronic applications.

Arrhenius analysis was used to estimate activation energy for charge transport[19]. Robertson's relation indicates an increase in carbon cluster parameters with irradiation dose, reflecting structural disorder. These changes enhance optical conductivity and dielectric performance, as summarized in Table 2.

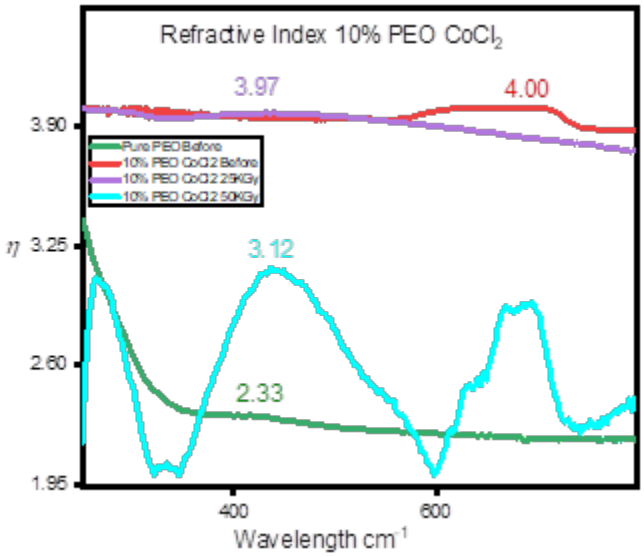


Fig 5. Refractive index variation with γ-irradiation dose for $CoCl_2$-doped PEO films.

Table 2. Optical parameters of pure and $CoCl_2$-doped PEO films under different γ-irradiation doses.

Samples	Absorption Coefficient (eV)	Extinction Coefficient (10^{-5})	Direct Band Gap (eV)	Indirect Band Gap (eV)	Refractive index
Pure PEO	2.27	11.07	4.05	2.99	2.33
10% Before	3.36	3.41	1.78	2.00	4.00
10% 25KGy	2.53	1.53	1.30	1.70	3.97
10% 50KGy	2.07	0.468	1.18	1.51	3.12

3.4 Electrical and Dielectric Analysis

AC conductivity studies were performed to investigate the charge transport behavior and dielectric response of the prepared films. Impedance spectroscopy was used to evaluate the dielectric constant, dielectric loss, and bulk resistance. The Nyquist plots (Fig.6), representing real (Zr) versus imaginary (Zi) impedance, provide insight into the resistive and capacitive characteristics of the system [20]. The zigzag nature of the Nyquist plot for pure PEO is due to its very high bulk resistance and extremely low ionic conductivity, which make the impedance measurements more susceptible to electrical noise and instrumental fluctuations. Upon $CoCl_2$ doping and gamma irradiation (25 and 50 kGy), the ionic conductivity increases significantly, resulting in smoother and well-defined Nyquist plots.

The bulk resistance (Rb), obtained from the intercept on the real axis, decreases significantly upon $CoCl_2$ doping and shows further variation with γ-irradiation, as summarized in Table **??**. This reduction indicates enhanced ionic conductivity due to increased charge carrier density and improved mobility. Additionally, the decrease in interfacial resistance suggests the formation of more efficient conduction pathways within the polymer matrix [21].

The frequency dependence of the dielectric constant (ε'), calculated using Eq. (9),

$$\varepsilon_r = \frac{Z_i}{2fC_oZ^2} \tag{9}$$

is shown in Figure 7.

The dielectric constant exhibits higher values at low frequencies (10^2–10^3 Hz), attributed to space charge polarization (Maxwell–Wagner–Sillars effect) [22], where charge carriers accumulate at interfaces in the heterogeneous system. As the frequency increases, ε' decreases due to the inability of dipoles to follow the rapidly alternating electric field. The increase

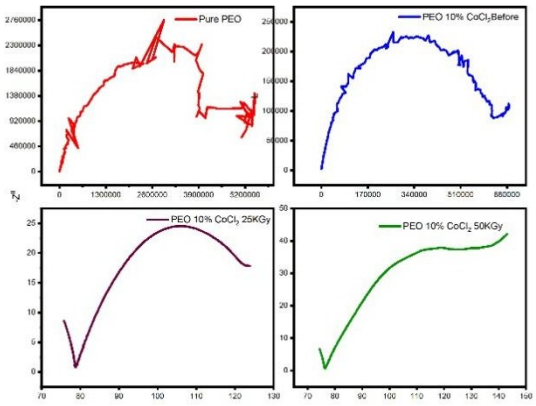


Fig 6. Nyquist plots of 10 wt% $CoCl_2$-doped PEO films at 25 kGy and 50 kGy γ-irradiation doses.

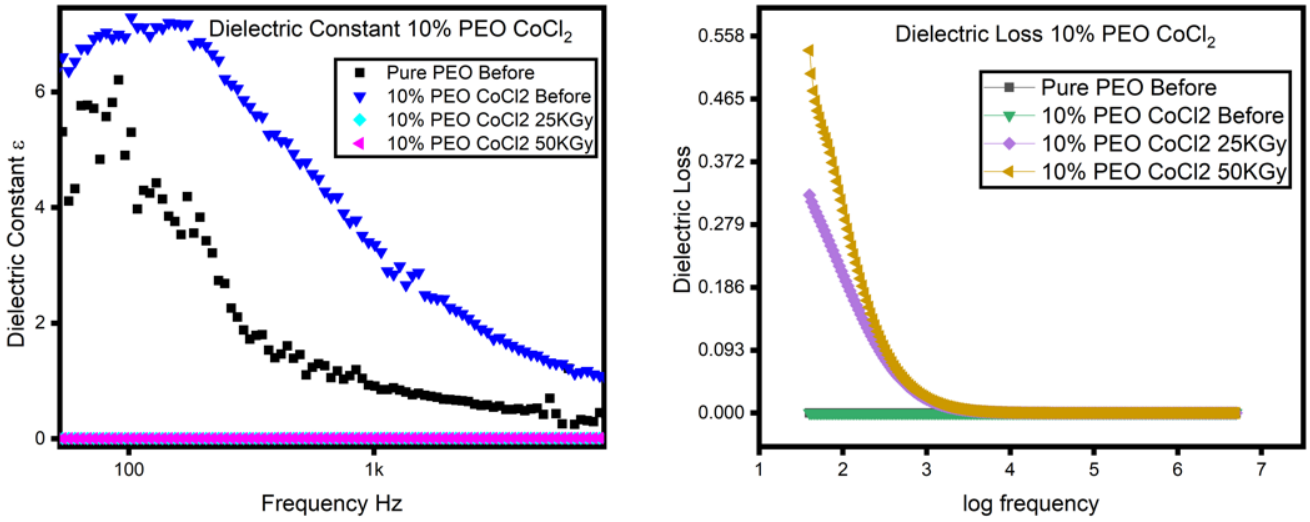


Fig 7. Frequency-dependent dielectric constant (ε') and Dielectric loss (ε'') of 10 wt% $CoCl_2$-doped PEO films under γ-irradiation at 25 kGy and 50 kGy.

in ε' with $CoCl_2$ doping is associated with enhanced polarization resulting from metal ion–polymer interactions and defect formation. Further enhancement in ε' upon γ-irradiation is attributed to chain scission, increased defect density, and formation of carbon clusters, leading to higher dipolar activity[23],[24]. Gamma irradiation creates localized defect states through chain scission, partial cross-linking, and the formation of carbon-rich clusters, thereby reducing the optical band gap. The XRD and FTIR results confirm that the polymer matrix remains structurally intact, indicating that the observed band gap reduction is attributed to irradiation-induced structural modifications.

The dielectric loss calculated using equation (10),

$$\varepsilon_i = \frac{Z_r}{2fC_oZ^2} \tag{10}$$

The dielectric loss (ε''), shown in Figure 7, is higher at low frequencies due to electrode polarization and charge carrier motion, and decreases at higher frequencies, indicating reduced energy dissipation. $CoCl_2$ doping enhances polarization through ion–polymer interactions, while γ-irradiation introduces defects and localized states that facilitate hopping conduction. These combined effects increase charge carrier mobility, improve dielectric response, and enhance overall electrical conductivity, confirming the suitability of $CoCl_2$-doped PEO films for flexible electrode and energy storage applications.

4 Conclusion

This study demonstrates a synergistic approach combining $CoCl_2$ doping and γ-irradiation to PEO for tailor the structural, optical, and electrical properties of PEO-based flexible films. Structural analyses (XRD and FTIR) inspects a transition from semicrystalline to amorphous phases, along with bond modifications such as d-spacing decreases to 6.48A0, FWHM reduces from 0.204 to 0.144, FTIR confirming amorphization in irradiated films and the formation of polymer–salt complexes (Co–O and Co–Cl) induced by chain scission and defect generation. Optical studies reveal a significant reduction in band gap (down to 1.30 eV) along with red shifted absorption, indicating enhanced electronic transitions and improved optical response. Electrical measurements show increased AC conductivity (10^{-} S cm^{-1}), higher dielectric constant, and reduced bulk resistance, confirming improved charge carrier mobility and polarization behavior. Nyquist analysis supports improved charge transport behavior through reduced impedance and conducts mechanism.

These enhancements are attributed to irradiation-induced defects and increased structural disorder, which facilitate hopping conduction within the polymer matrix. Overall, the results highlight γ-irradiation as an effective strategy for tuning polymer electrolyte properties.

Thus, this work is achieved in establishing a quantitively correlation between γ-irradiation flexible films for low-power electronics, radiation tolerant optoelectronic devices, polymer sensors. The developed γ-irradiated $CoCl_2$-doped PEO films exhibit promising performance for applications in flexible electrodes, energy storage devices, and optoelectronic systems, particularly in radiation-prone environments. The future work focus on varied dopant concentration with γ-irradiation dose, thin film to maximize conductivity, advance the practical implementation of these to next generation electronic gadgets.

5 Acknowledgments

The authors acknowledge Sahyadri Science College, Kuvempu University, for fabrication facilities. Appreciation is extended to Dr. Praveen K. C. (LEOS– ISRO) for UV-NIR spectroscopy, Prof. Ganesh Sanjeev (Mangalore University) for AC conductivity studies, and Prof. Balram Sahoo (IISc Bangalore) for XRD analysis.

References

1) Lu X, Zhang Y, Zheng Z. Metal-Based Flexible Transparent Electrodes: Challenges and Recent Advances. *Advanced Electronic Materials*. 2021;7:2001121. https://doi.org/10.1002/aelm.202001121.
2) Zhang C, Ji C, Park YB, Guo LJ. Thin-Metal-Film-Based Transparent Conductors: Material Preparation, Optical Design, and Device Applications. *Advanced Optical Materials*. 2021;9:2001298. https://doi.org/10.1002/adom.202001298.
3) Johari SNAM, Tajuddin NA, Hanibah H, Deraman SK. Ionic Conductivity of Solid Polymer Electrolyte Based Polyethylene Oxide. *International Journal of Electrochemical Science*. 2021;16:210053. https://doi.org/10.20964/2021.10.53.
4) Armand M, Tarascon JM. Building Better Batteries. *Nature*. 2008;451:652–657. https://doi.org/10.1038/451652a.
5) Chapi S. Influence of Co^{2+} on the Structure and Conductivity of PEO-Based Electrolytes. *Journal of Electronic Materials*. 2021;50:1558–1571. https://doi.org/10.1007/s11664-020-08706-6.
6) Anyaogu ID, Nwanya AC, Ezema FI, Ejikeme PMC. Cobalt Ion-Doped Polymer Electrolyte for Aluminium–Air Battery Application. *Hybrid Advances*. 2025;8:100369. https://doi.org/10.1016/j.hybadv.2024.100369.
7) Algethami M. Optical Investigation of Gamma Radiation Effects on PVA/CS/CMC Blend Membranes. *Journal of Radiation Research and Applied Sciences*. 2025;18:101812. https://doi.org/10.1016/j.jrras.2025.101812.
8) Madhukumar R, et al. Influence of Ionizing Radiation on Biosynthesis of Noble Metal Nanoparticles and Applications. *Indian Journal of Science and Technology*. 2025;18:1792–1800. https://doi.org/10.17485/IJST/v18i22.3428.
9) Gowtham GK, Urs TG. Structure-Dependent Optical and Conductive Properties of HPMC:$CoCl_2$ Composites. *AIP Advances*. 2025;15:015001. https://doi.org/10.1063/5.0237654.
10) Udayaraj S, Annappa M, Roopa KV, Mathad G, Subramanya K, Pavithra GM. Optical, Structural and Conductivity Properties of Ferrous Sulfate Doped Polyaniline. *Materials Today: Proceedings*. 2023;p. 132–138. https://doi.org/10.1016/j.matpr.2023.05.384.
11) Telfah A, et al. Optical, Electrical and Chemical Properties of PEO:I_2 Composite Films. *Polymer Bulletin*. 2023;80:9611–9625. https://doi.org/10.1007/s00289-022-04508-4.
12) Yang R, et al. Coenzyme-Based Elastomeric Adhesive Patch for Iron Regulation. *Bioactive Materials*. 2026;55:224–240. https://doi.org/10.1016/j.bioactmat.2025.09.019.
13) Mondal S, Sen S, Kumar A, Mudila H. Modulation of Optical Band Gap and Conductivity of Polyindoles. *Results in Optics*. 2023;13:100556. https://doi.org/10.1016/j.rio.2023.100556.
14) Sudhakar K, Venugopal R, Narsimlu N, Srinivas CH. CuO-Incorporated PEO Nanocomposite Films for Optoelectronics. *Journal of Physics: Conference Series*. 2024;2778:012010. https://doi.org/10.1088/1742-6596/2778/1/012010.
15) Patel D, et al. A Review on UV Visible Spectroscopy. *International Journal of Creative Research Thoughts*. 2022;10. Available from: https://ijcrt.org/papers/IJCRT2210171.pdf.
16) Agrahari S, et al. A DFT Based Investigation of Structural and Optoelectronic Properties of Solid Polymer Electrolyte LiFSI Complexes. *Research Square*. 2024. https://doi.org/10.21203/rs.3.rs-4675980/v1.
17) Patil A, Patil N. Synthesis, Characterization and Conductance Properties of Cobalt Chloride Doped Polyvinyl Alcohol / Polythiophene (PVA-Co-Pth) Nanocomposite Films. *Journal of Materials Science and Surface Engineering*. 2022;9. https://doi.org/10.52687/2348-8956/912.

18) Perera IN, et al. Enhanced Electrochemical Properties of Cobalt by Varying the Ethylene Glycol - Choline Chloride Composition in a Deep Eutectic Solvent Mixture. *Journal of The Electrochemical Society*. 2023;170. https://doi.org/10.1149/1945-7111/acd02a.
19) Doremus JG, et al. Photocatalytic applications of covalent organic frameworks: synthesis, characterization, and utility. *Nanoscale*. 2024. https://doi.org/10.1039/D4NR03204G.
20) Guzman-Puyol S, et al. Transparency of polymeric food packaging materials. *Food Research International*. 2022. https://doi.org/10.1016/j.foodres.2022.111792.
21) Charradi K, et al. Fabrication and Characterization of Polyvalent Metals/Oxidized Polyvinyl Alcohol Hybrid Films with Improved Proton Conductivity and Optical Performances. *Journal of Polymers and the Environment*. 2023;31. https://doi.org/10.1007/s10924-023-02824-y.
22) Tüfekçi M, et al. Long-term antifouling surfaces for urinary catheters. *Journal of Materials Chemistry B*. 2024. https://doi.org/10.1039/D4TB00311J.
23) Anula MS, BeskeyJob C. Growth, Spectral, Optical, Thermal, Mechanical and Dielectric properties of CdCl2 added (Na)2 SbF5 Single Crystals. *Journal of Pharmaceutical Negative Results*. 2023. https://doi.org/10.47750/pnr.2023.14.02.299.
24) Zahir MH, et al. Shape - Stabilized Phase Change Materials For Energy Storage. *United States Patent Application Publication*. 2021. Available from: https://patents.google.com/patent/US20210102106A1/en.